

Understanding RF-Specific Plasma–Material Interaction and Whole-Device Impurity Transport in High-Power Helicon Operation on DIII-D

DIII-D has recently demonstrated high-power helicon operation[1] as a promising RF system for mid-radius current drive. As with other high-power RF systems, helicon operation in DIII-D can potentially introduce new plasma–material interaction (PMI) challenges near antenna structures. Rectified RF sheaths can accelerate scrape-off-layer ions to multi-keV energies, enhancing sputtering and generating localized impurity sources that may increase radiative losses and contribute to core contamination, particularly for future high-Z plasma-facing components.

To quantify RF-driven PMI, we analyze two DIII-D H-mode discharges with antenna–plasma gaps of 7 cm and 4 cm and coupled RF powers of 0.15 MW and 0.25 MW using STRIPE, an integrated modeling framework for RF-PMI[2], [3]. The 30-element traveling-wave antenna in DIII-D operates at 476 MHz with a spectrum peaked near $n_{||} \approx 3$. In the low-density edge region, slow-wave accessibility may generate finite parallel electric fields that could drive strong RF sheath rectification along open magnetic field lines.

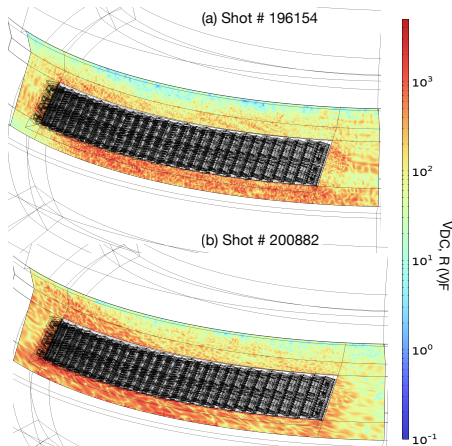


Figure 1: 3D RF sheath potential distribution near the helicon antenna. Rectified sheath potentials of 2–5 kV localize where magnetic field lines intersect surfaces at grazing angles.

STRIPE combines experimentally constrained SOLPS-ITER background plasmas (validated with Thomson and helium beam diagnostics) with 3D COMSOL sheath simulations using a dielectric-layer model. Sheath-accelerated ion distributions from GITER are coupled with RustBCA sputtering yields to compute erosion, and the resulting impurity sources are evolved with 3D whole-device transport simulations using GITRM.

Simulations predict rectified sheath potentials of 2–5 kV, increasing ion impact energies, particularly near the lower antenna where field lines intersect surfaces at grazing angles. Carbon erosion is dominated by self-sputtering, with effective yields approaching ~ 8 atoms/ion, while RF-accelerated D^+ contributes $\sim 1\%$ of the total erosion flux. Reducing the antenna–plasma gap increases sheath-connected area and plasma accessibility, producing more than an order-of-magnitude rise in gross erosion.

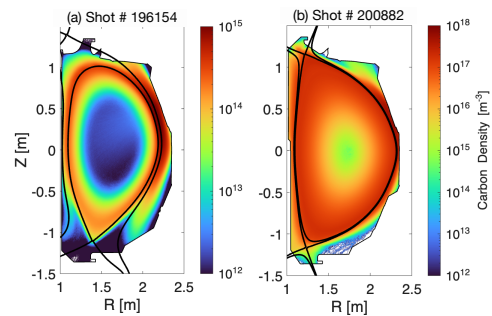


Figure 2: Whole-device impurity density distribution from GITRM. Reduced antenna–plasma gap enhances core penetration of helicon-sourced carbon ($\sim 58\%$ vs $\sim 35\%$).

Whole-device modeling shows strong sensitivity to antenna–plasma separation, with $\sim 58\%$ of helicon-sourced carbon penetrating inside the separatrix for the smaller-gap discharge compared to $\sim 35\%$ for the larger-gap case. The helicon antenna carbon source remains well below the divertor source and does not measurably change the global carbon inventory, consistent with experiment. However, under tighter coupling, higher RF power, or future high-Z walls, even modest main-chamber impurity sources could increase core radiation and impact confinement.

References

- [1] R. Pinsker *et al.*, “First high-power helicon results from diii-d,” *Nuclear Fusion*, vol. 64, no. 12, p. 126 058, 2024.
- [2] A. Kumar *et al.*, “Integrated modeling of rf-induced tungsten erosion at icrh antenna structures in the west tokamak*,” *Nuclear Fusion*, vol. 65, p. 076 039, 2025.
- [3] Kumar, Atul *et al.*, “Analysis of rf sheath-driven tungsten erosion at rf antenna in the west tokamak,” *EPJ Web Conf.*, vol. 346, p. 01 004, 2026.